

# Three-Dimensional System for the *In Vitro* Study of Megakaryocytes and Functional Platelet Production Using Silk-Based Vascular Tubes

Isabella Pallotta, Ph.D.,<sup>1,2</sup> Michael Lovett, Ph.D.,<sup>1</sup> David L. Kaplan, Ph.D.,<sup>1</sup> and Alessandra Balduini, M.D.<sup>1,2</sup>

Platelets are specialized cells produced by megakaryocytes in the bone marrow that represent the first defense against hemorrhage, yet they also play a pathological role in thrombosis, inflammation, and cancer. Millions of platelet transfusions are conducted each year, and the supply of this blood component is limited. There are many diseases where platelet production or function is impaired with severe consequences for patients. With such clinical need, new insight into the formation of platelets would have a major impact on patients and healthcare. We developed an innovative 3D system to study platelet production that represents the first spatial reconstruction of the bone marrow environment. In this system human megakaryocytes were able to migrate toward the vascular niche, extend proplatelets, and release functional platelets into vascular tubes. The combination of different bone marrow components and the compliance of silk-based vascular tubes makes this model a unique tool for the study of platelet formation and production for use in healthcare needs.

## Introduction

**T**HE BONE MARROW represents a challenging human organ to study due to its structure and complexity within the bone cavity. Therefore, mechanisms that regulate hematopoietic stem cell homing, proliferation, and differentiation within the bone marrow environment are still undefined. Among these, an open question is how bone marrow and vascular niches impact platelet formation, a key feature in many aspects of human physiology. The approximate lifespan of each platelet is 10 days<sup>1</sup>; therefore, the platelet supply needs to be continually renewed by differentiation of progenitors. Thrombocytopenia is a major clinical problem encountered across a number of conditions including different hematological diseases as well as chemotherapy treatments or cardiac surgery. Thrombocytopenia often requires platelet transfusions for patients. The availability of this blood component is limited and varies depending on the availability of donors.<sup>2</sup> The most recognized model of platelet formation provides that it occurs in the bone marrow where megakaryocytes migrate from the osteoblastic to the vascular niche and then extend long filaments, called proplatelets, that protrude through the vascular endothelium into the sinusoid lumen, where the platelets are released.<sup>3,4</sup> Physiological evidence of proplatelet formation has been demonstrated by electron microscopy analysis<sup>5</sup>; more recently, proplatelet formation and platelet release have been

shown by multiphoton intravital microscopy in intact bone marrow from mice.<sup>6</sup> Further studies are underway to exploit new strategies to generate platelets for clinical transfusion and studies of thrombopoiesis.<sup>7</sup> These include functional platelets derived *in vitro* from selected induced pluripotent stem cells (iPSC) clones<sup>8</sup> and infused megakaryocytes generating functional platelets, *in vivo*, in mice.<sup>9</sup> Finally, different proteins, such as fibrinogen (FBG) or von Willebrand factor (vWF), are known to support megakaryocyte maturation and proplatelet formation.<sup>10,11</sup> However, many aspects regarding the mechanisms underlying proplatelet extension and platelet release remain unsolved, especially in humans.<sup>12</sup> Specifically, insight is needed on how the microenvironment surrounding megakaryocytes regulates platelet formation.<sup>13,14</sup> Building upon our recently established vascular systems,<sup>15,16</sup> a 3D gel network was adapted to reproduce a bone marrow environment<sup>17</sup> and used to study megakaryocyte function toward platelet production as outlined in Figure 1.

## Materials and Methods

### Materials

*Bombyx mori* silkworm cocoons were supplied by Tajima Shoji Co., Ltd. (Yokohama, Japan). Stainless steel wire, Type 304V, was supplied by Small Parts (Miami Lakes, FL). Pharmed tubing was from Cole-Parmer (Vernon Hills, IL). Type I rat tail collagen was from Upstate Cell Signaling

<sup>1</sup>Department of Biomedical Engineering, Tufts University, Medford, Massachusetts.

<sup>2</sup>Biotechnology Research Laboratories, Department of Biochemistry, IRCCS San Matteo Foundation, University of Pavia, Pavia, Italy.

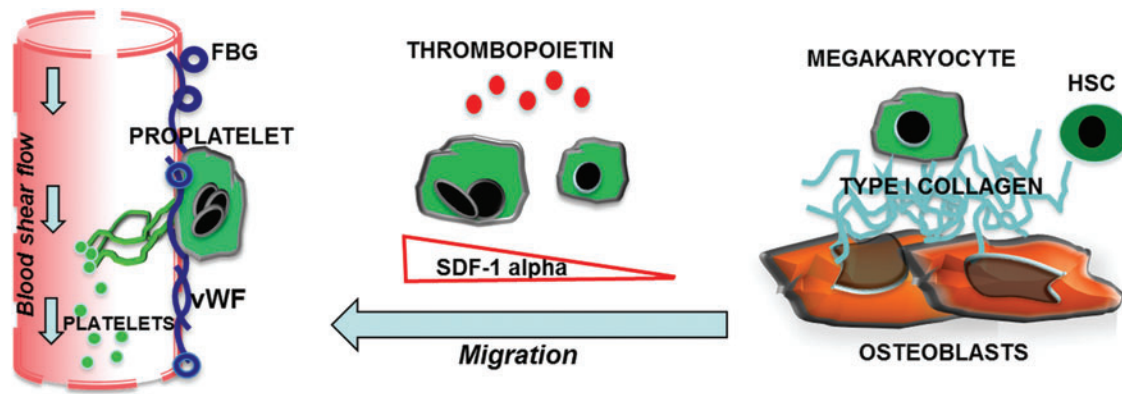


**FIG. 1.** Outline of platelet formation in the bone marrow environment. Immature megakaryocytes in contact with the osteoblastic niche are inhibited in their maturation. Upon migration toward the vascular niche, megakaryocytes extend proplatelets and release platelets into the blood stream. Interactions of megakaryocytes with matrices supposed to fill the vascular niche, such as fibrinogen (FBG) or von Willebrand factor (vWF), are able to sustain proplatelet formation, whereas type I collagen, in the osteoblastic niche, totally suppresses this event and prevents premature platelet release. SDF-1 $\alpha$  is produced locally by the stromal cells and promotes the migration and contact of megakaryocytes with the permissive vascular niche. Color images available online at [www.liebertonline.com/tec](http://www.liebertonline.com/tec)

Solutions (Lake Placid, NY), Matrigel from BD Pharmingen (San Diego, CA), FBG and calcein-AM from Sigma (St. Louis, MO), and vWF (Haemate P) from Aventis-Behring (Milan, Italy). Lympholyte was from Accurate Chemical and Scientific Corporation (New York). Immunomagnetic separation system was from Miltenyi Biotech (Auburn, CA). Stem Span medium was from Stem-Cell Technologies (Vancouver, Canada). Recombinant human thrombopoietin (TPO), interleukin (IL)-6, IL-11, and SDF-1 $\alpha$  were from PeproTech (Rocky Hill, NJ). The following antibodies have been used: mouse monoclonal anti-CD61, clone SZ21, from Immunotech (Marseille, France); mouse anti-tubulin, clone DM1A, from Sigma; and PE mouse anti-human CD41a, FITC mouse anti-human CD62P, PE mouse anti-human CD42b, and PAC1-FITC from BD Pharmingen. Alexa Fluor 488-conjugated chicken anti-mouse, Mowiol 4-88 and Hoechst 33258 were from Molecular Probes (Eugene, OR).

#### Bioreactor design adapted to megakaryocyte function

The recently established bioreactor platform<sup>15,16</sup> was adapted to combine several features of the bone marrow environment to study the key steps of megakaryocyte development such as migration from the osteoblastic to the vascular niche, contact with the vascular environment, proplatelet extension, and platelet release (Fig. 2A). Bioreactors consist of 3 wells (10 $\times$ 15 $\times$ 5 mm) within a PDMS block (25 $\times$ 60 $\times$ 5 mm), which is plasma bonded to cover glass (Goldseal, No. 1, 24 $\times$ 60 mm; Ted Pella, Redding, CA) for imaging. Briefly, in each well a stainless steel rods (0.025" diameter), was positioned  $\sim$ 500  $\mu$ m from the bottom edge of the bioreactor and embedded in the PDMS during the pouring and curing process. Once removed, 23 G stainless steel needles were used to perfuse the porous silk microtubes.

#### Preparation of silk microtubes

Silk fibroin aqueous solution was obtained from *B. mori* silkworm cocoons using previously described proce-

dures.<sup>15,18,19</sup> Silk microtubes were then prepared by dipping stainless steel wire (0.64 mm) into 14%–16% (w/v) silk fibroin.<sup>15</sup> Briefly, when the stainless steel rods were evenly coated with concentrated silk fibroin, they were then dipped into methanol, inducing a transformation in the concentrated silk fibroin from an amorphous liquid to the beta sheet-form. The process of alternate dipping in concentrated aqueous silk fibroin solution and methanol was carried out until the stainless steel wire was evenly coated (2–4 times) to obtain silk tubes around 50 $\pm$ 20  $\mu$ m of thickness to accommodate the entire length of proplatelets and allow proplatelet extension through the vascular tube wall (Fig. 2Bi-ii). To allow proplatelet passage through the walls,<sup>20</sup> defined pore sizes of 2–8  $\mu$ m were obtained by adding 6 w/t% poly(ethylene oxide) (PEO) to the silk fibroin to achieve a 98.5/1.5 wt% silk fibroin/PEO blend. The silk/PEO tubes were dipped and treated as described above and left to dry overnight before being cut at each end and placed in a surfactant solution to remove the silk microtube from the steel wire. Tubes were then soaked in distilled water over 24 h to extract the PEO from the tube, which resulted in a porous silk tube (Fig. 2Ci). Pore interconnections were shown along the entire depth of the wall, leaving several paths through which the proplatelets could extend (Fig. 2C ii). Before any cell-based experiments, the microtubes were sterilized in 70% ethanol.

#### Characterization of silk microtubes:

##### Scanning electron microscopy

The pore size distribution in the silk microtubes, as well as the interconnectivity through the entire wall of the silk microtubes, were analyzed using a Carl Zeiss (Carl Zeiss SMT, Germany) Ultra 55 field emission scanning electron microscopy (FESEM) system operating at an accelerating voltage of 5 kV and using an in-lens ion annular secondary electron detector at Harvard University Center for Nanoscale Systems (Cambridge, MA). The scaffolds were coated with platinum/palladium for 1 min before SEM observation.

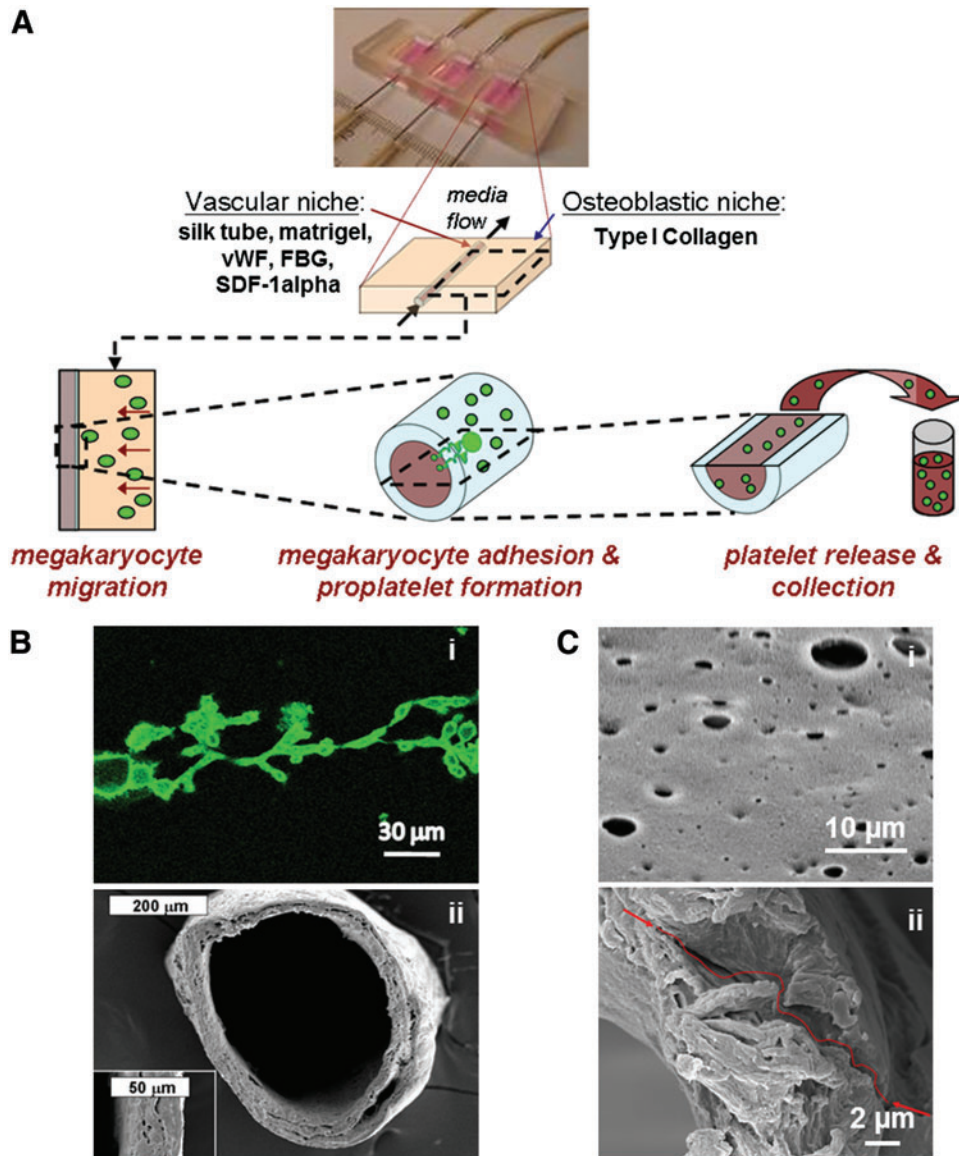


**FIG. 2.** Bioreactor platform and silk microtubes. **(A)** The previously developed bioreactor platform was adapted to reproduce the bone marrow microenvironment to study megakaryocyte migration, adhesion to the sinusoidal vessel, proplatelet formation, and platelet release. **(B)** Scanning electron microscopy (SEM) image of a representative silk microtube used to mimic blood vessels **(ii)**. The wall thickness was adjusted around 50  $\mu\text{m}$  to match proplatelet length **(i)**. **(C)** To allow proplatelet elongation through the vascular microtube wall, defined pore sizes of 2–8  $\mu\text{m}$  were obtained as described in Materials and Methods. **(i)** SEM image of vascular microtube wall pores. **(ii)** SEM image showing pore interconnection and a path through the tube wall. Color images available online at [www.liebertonline.com/tec](http://www.liebertonline.com/tec)

#### Preparation of matrices in the bioreactor

Before positioning, silk tubes were coated with SDF-1 $\alpha$  (300 ng/mL) and Matrigel diluted or not with vWF (1 mg/mL) to a final concentration of 25  $\mu\text{g}/\text{mL}$  or FBG (12 mg/mL) to a final concentration of 4 mg/mL or type I collagen (from bovine tendons, generously donated by Maria Enrica Tira, Department of Biochemistry, University of Pavia, Pavia, Italy) to a final concentration of 25  $\mu\text{g}/\text{mL}$ , and incubated for 30 min. Collagen gels were prepared on ice by mixing 1.22 mL type I rat tail liquid collagen (4 mg/mL in 0.02 N acetic acid, 12.2  $\mu\text{L}$  2 M sodium hydroxide, 20  $\mu\text{L}$  100 mM ascorbic acid, and 768  $\mu\text{L}$  of growth medium for a final collagen concentration of  $\sim 1$  mg/mL). This collagen suspension was then distributed at the borders of each well of the bioreactor and maintained at 25°C for 15–30 min to allow for even gelation before being placed in the incubator. To adjust the gel thickness based on the spatial distribution of blood vessels with respect to bone into the bone marrow environment,<sup>21</sup> a cover glass was positioned  $\sim 150$   $\mu\text{m}$  from the silk

microtube to allow the separation of the Matrigel-coated silk tube and the collagen gel composition.

#### Megakaryocyte cultures

Human umbilical cord blood was purchased from The National Disease Research Interchange (Philadelphia, PA). Human umbilical cord blood CD34<sup>+</sup> cells were separated and cultured as previously described.<sup>10</sup>

Briefly, CD34<sup>+</sup> cells were separated by immunomagnetic beads (purity >90%) and cultured for 12 days in Stem Span medium supplemented with 10 ng/mL TPO, IL-6, and IL-11, in the presence of 1% penicillin–streptomycin at 37°C in a 5% CO<sub>2</sub> fully humidified atmosphere. The medium was changed at day 3, 7, and 10 of culture. For 3D experiments, at day 12 of differentiation mature megakaryocytes not yet exhibiting proplatelets were stained with an anti-CD61 antibody for 45 min at 37°C, washed 3 times with phosphate-buffered saline (PBS), and incubated with 10 mg/mL of the secondary antibody conjugated with Alexa Fluor 488 in PBS for 1 h at



37°C. Subsequently,  $3 \times 10^5$  megakaryocytes were resuspended in Stem Span medium, 10 ng/mL TPO, and 100 U/mL penicillin–streptomycin, and added to each well of the bioreactor at the interface between the collagen I gel and the coated silk tube upon the removal of the cover glass (as above reported), and maintained at 37°C in a 5% CO<sub>2</sub> fully humidified atmosphere, before analyzing migration toward the silk microtubes, adhesion to the silk tubes, proplatelet formation through the silk microtube, and platelet release inside the microtube by confocal microscopy.

For 2D experiments, at day 13 of differentiation, megakaryocytes were reseeded in a 24-well plate ( $3 \times 10^5$  megakaryocytes/well) in Stem Span medium supplemented with 10 ng/mL TPO and 100 U/mL penicillin–streptomycin. Released platelets were collected after 16 h and processed as described below.

For controls, human peripheral blood platelets were separated and treated as collected platelets. Briefly, human platelets were obtained from healthy volunteers in sodium citrate. Whole blood was centrifuged at 150 *g* for 10 min to obtain platelet-rich plasma (PRP). Prostaglandin I<sub>2</sub> (1 μM) was added to the PRP. Platelets were recovered by centrifugation at 720 *g* for 15 min, washed with 10 mL of PIPES buffer (20 mM PIPES and 137 mM NaCl, pH 6.5), and finally gently resuspended in Tyrode buffer (134 mM NaCl; 0.34 mM Na<sub>2</sub>HPO<sub>4</sub>; 2.9 mM KCl; 12 mM NaHCO<sub>3</sub>; 20 mM HEPES; pH 7.0; 5 mM glucose; 0.35% [w/v] bovine serum albumin [BSA]).

#### *Confocal analysis of megakaryocyte migration, megakaryocyte forming proplatelet, and released platelets in 3D*

After 16 h, fluorescence images of megakaryocytes migrated through the different gels were acquired using a Leica DMIRE2 confocal microscope with a TCS SP2 scanner (Leica Microsystems, Mannheim/Wetzlar, Germany). Sections of 400 μm were acquired through a 20× objective. After 24 h, megakaryocyte adhesion to the external wall of the silk microtubes, proplatelet formation through the wall of the tubes, and released platelets within the silk microtube were analyzed via confocal analysis through a 63× objective by using the same equipment.

#### *Perfusion of silk microtubes*

To collect platelets released from megakaryocyte forming proplatelets through the silk tubes, the bioreactor was perfused with Stem Span medium supplemented with sodium citrate (10 μM) and 100 U/mL penicillin–streptomycin. This solution was then perfused using a remote push–pull syringe pump (Harvard Apparatus, Holliston, MA), programmed to flow at a rate of 32 μL/min into the silk microtubes for 16 h before collecting the effluent medium. Flow rate was determined by taking into account the flow shear rate in capillaries around 32/s<sup>22</sup> and using the following equation for the shear rate at the inner wall of a Newtonian fluid flowing within a pipe:<sup>23</sup>

$$\gamma = \frac{8v}{d},$$

where

$\gamma$  = The shear rate, measured in reciprocal seconds.

$v$  = The linear fluid velocity, measured in meters per second.

$d$  = The inside diameter of the pipe, measured in meters.

The linear fluid velocity  $v$  is related to the volumetric flow rate  $Q$  by:

$$v = \frac{Q}{A}$$

$A$  is the cross-sectional area of the pipe, which for an inside pipe radius of  $r$  is given by:

$$A = \pi r^2,$$

thus producing

$$v = \frac{Q}{\pi r^2}$$

#### *Flow cytometry analysis of collected platelets*

After bioreactor perfusion and 2D cultures, size, integrity, and functionality of collected platelets were analyzed by flow cytometry. Briefly, collected cells were centrifuged at 720 *g* for 15 min and stained with 8 μL of an antibody against CD41 in 100 μL of Tyrode buffer for 30 min. Platelets isolated from human peripheral blood were used as a positive control. Collected platelets after perfusion or *in vitro* released platelets collected at day 14 of culture were analyzed using the characteristic forward and side scatter pattern and fluorescence intensity of human peripheral blood platelets. To exclude cellular fragments, platelets were double-stained with 2 μL of calcein-AM and 8 μL of an anti-CD41PE antibody. Samples were analyzed using a FACSCalibur flow cytometer. Irrelevant isotype-matched controls directly conjugated to FITC or PE were used to assess nonspecific fluorescence. To analyze platelet functionality, CD62P expression and PAC-1 binding in response to thrombin activation were assessed. Collected cells were centrifuged at 720 *g* for 15 min with PGI<sub>2</sub> to avoid platelet preactivation and then resuspended in Tyrode buffer and left to rest for 30 min at 37°C. The suspension was stimulated with 3 U/mL thrombin for 3 min at 37°C. Anti-P-selectin-FITC and anti-CD41-PE antibodies or mAb PAC-1-FITC, recognizing the activated αIIbβ<sub>3</sub> receptor, in combination with an anti-CD42b-PE, were added for 30 min. P-selectin expression and PAC-1 binding were measured by flow cytometry, using the characteristic forward and side scatter pattern and fluorescence intensity of human peripheral blood platelets.

#### *Immunofluorescence analysis of collected platelets*

Morphology of collected platelets in the flow effluent and in 2D culture was analyzed by immunofluorescence assay. Collected platelets were cytospun onto glass coverslips and fixed in 3% paraformaldehyde for 20 min at room temperature (RT). Upon washing with PBS, cells were blocked with 3% BSA in PBS for 1 h at RT. Platelets were then incubated for 1 h at RT with the primary monoclonal antibody mouse anti-tubulin, 1:500, diluted in PBS. After washing with PBS, cells were incubated with 10 mg/mL of the secondary antibody conjugated with Alexa Fluor 488 in PBS for 1 h at RT.

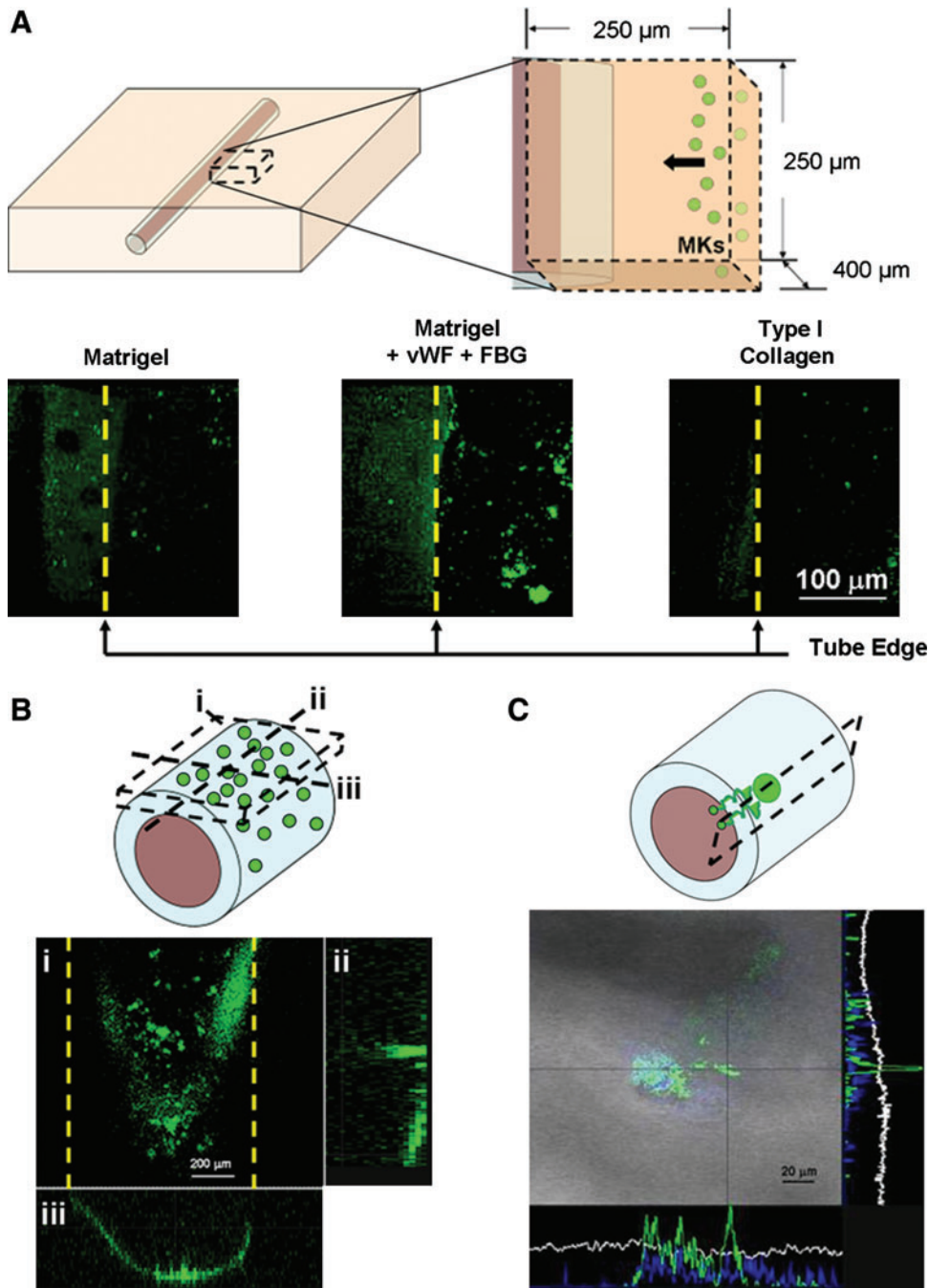


**FIG. 3.** Megakaryocyte migration, adhesion, and proplatelet formation. Mature megakaryocytes were stained with an anti CD61 antibody and added to each well of the bioreactor. **(A)** The silk microtubes were coated with 300 ng/mL SDF-1 $\alpha$  and a combination of Matrigel with FBG and vWF or Matrigel alone or type I collagen, as controls. Prestained megakaryocytes were then added to each bioreactor and megakaryocyte migration toward the vascular microtubes was analyzed. After 16 h megakaryocyte migration through the gel composed of Matrigel + FBG + vWF was significantly higher compared with other conditions. **(B)** Z-stack projection **(i)** of megakaryocytes in adhesion to the surface of the silk microtube well after 24 h incubation with orthogonal projections in the z-y **(ii)** and x-z **(iii)** directions to confirm cell adhesion in tube cross-sections. **(C)** After an additional 16 h, megakaryocytes extended proplatelets through the vascular microtube wall as shown in the orthogonal projections of a proplatelet (green) protruding into the vascular tube (gray). Color images available online at [www.liebertonline.com/tec](http://www.liebertonline.com/tec)

Nuclear counterstaining was performed with Hoechst 33258 (100 ng/mL) in PBS. Specimens were mounted in Mowiol 4–88. Images were acquired using an Olympus BX51 (Hamburg, Germany) microscope, through a 100 $\times$ /1.30 UplanF1 oil-immersion objective.

#### SEM of collected platelets

Spreading of collected platelets in 2D and 3D cultures, as well as controls, was analyzed by SEM. Glass coverslips were coated with type I collagen 25  $\mu$ g/mL overnight at 4 $^{\circ}$ C or FBG 100 mg/mL for 2 h at RT. Collected platelets after bioreactor perfusion were preincubated with 3 U/mL thrombin and allowed to adhere and spread on protein-

coated coverslips at 37 $^{\circ}$ C for 30 min. Cells were then fixed in 2.5% glutaraldehyde for 30 min at RT and dehydrated through a series of alcohols. The samples were coated with platinum/palladium for 1 min and analyzed by SEM using an in-lens ion annular secondary electron detector.

#### Statistics

Values were expressed as mean  $\pm$  SD (standard deviation). Student's *t*-test was performed for paired observations. A value of  $p < 0.05$  was considered statistically significant. Statistical analysis was carried out using SigmaStat 3.0 software. All experiments were independently replicated at least three times, unless differently specified.

## Results

### *Megakaryocytes migrated into the recreated bone marrow environment of the bioreactor system*

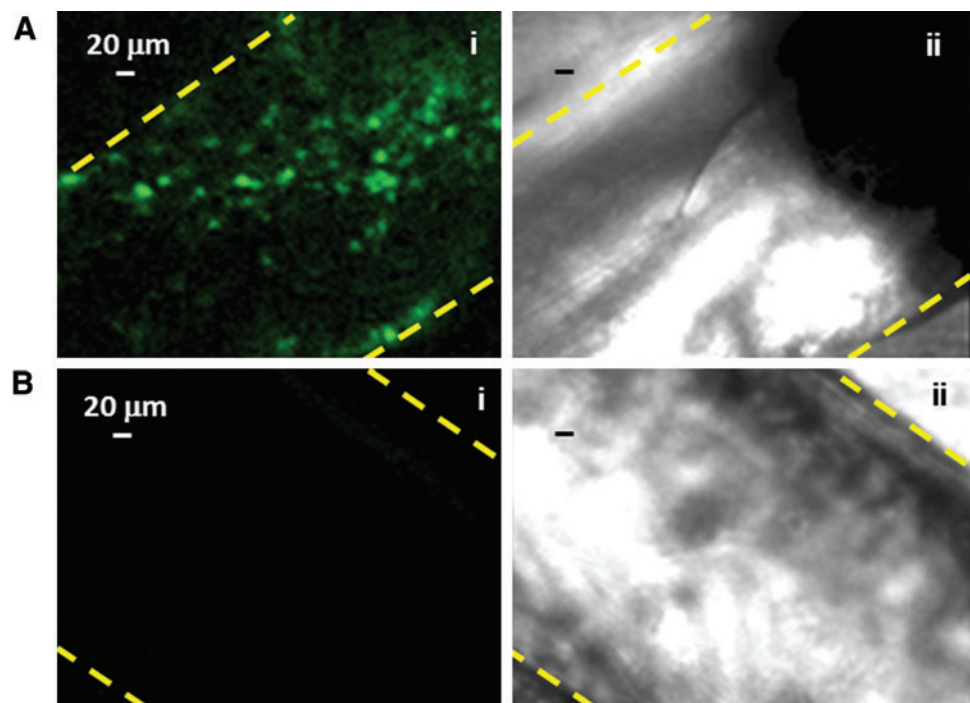
Migration through the 150  $\mu\text{m}$  thickness of the gel coating, toward the vascular tube, was observed using confocal microscopy. As shown in Figure 3A, after 16 h  $10\% \pm 5\%$  of the total megakaryocytes seeded were observed in the gel enriched with FBG and vWF, whereas only a few megakaryocytes were observed in the type I collagen gel or Matrigel alone. After an additional 8 h, migrated megakaryocytes in the gel enriched with FBG and vWF were observed on the external wall of the vascular microtubes by confocal microscopy (Fig. 3B). A time-course analysis demonstrated that 16 h was the time limit to start appreciating megakaryocytes into the gel coating, prolonging the incubation to 24 h affected only the position toward the vascular tube and not the number of migrated megakaryocytes (data not shown). Moreover, when vascular tubes were coated with either Matrigel alone or with type I collagen, prolonging incubation to 24 h did not affect megakaryocyte migration (data not shown). Because megakaryocyte migration in a 3D *in vitro* assay has never been studied before,<sup>24,25</sup> these results are the first to show that adhesive interactions with specific proteins drove megakaryocyte crawling toward the vascular space in the bioreactor environment.<sup>3,10,11</sup>

### *Megakaryocytes extended proplatelets and released functional platelets into the silk microtube flow*

Upon adherence onto the external wall of the vascular tube,  $7\% \pm 2\%$  of the megakaryocytes extended proplatelets over a 16-h incubation.<sup>10</sup> Figure 3C shows a representative analysis using confocal microscopy, of the orthogonal pro-

jections of a megakaryocyte extending proplatelets that protrude through the pores of the vascular wall. For megakaryocyte migration and perfused vascular tubes, the silk microtubes were perfused using a remote push-pull syringe pump at a rate of 32  $\mu\text{L}/\text{min}$ , corresponding to a shear rate of 40.9/s. In this case, platelets were observed inside the porous tubes (Fig. 4A), whereas no signals were detected in control non porous ones at the confocal microscopy analysis (Fig. 4B). The flow through of the vascular microtubes was collected and analyzed by flow cytometry, immunofluorescence, and SEM. Collected platelets were identified as cells having the same scatter properties and fluorescence intensity of normal human peripheral blood platelets and expressed CD41 (Fig. 5Ai). Consistent with the migration experiments, platelets were collected in the flow effluent only when the vascular microtubes were coated with Matrigel, FBG, and vWF (Fig. 5Aii). On the other hand, few platelets were collected from uncoated vascular microtubes and no platelets were observed after perfusion of type I collagen gel-coated microtubes (Fig. 5Aiii, iv). For the tubes coated with Matrigel, FBG, and vWF, the yield of collected platelets was  $200 \pm 50$  per megakaryocyte that extended proplatelets. To exclude cellular fragments, collected platelets were double stained with an anti-CD41 antibody and calcein-AM (Fig. 5B). The percentage of double-stained population was almost 50%, demonstrating that half of the collected cells were intact platelets.<sup>26</sup> Moreover, collected platelets displayed circumferential microtubule coils comparable to control, peripheral blood platelets, as demonstrated by anti-tubulin staining and immunofluorescence microscopy analysis (Fig. 5Ci, ii).<sup>4,12</sup> Further, collected platelets were shown to be functional by increased exposure of P-selectin to the plasma membrane upon stimulation with thrombin ( $65\% \pm 3.5\%$  (mean  $\pm$  SD,  $n=3$ ) (Fig. 5Dii). As compared to control, peripheral blood

**FIG. 4.** Released platelets inside silk microtubes are dependent on tube porosity. After staining megakaryocytes with an anti-CD61 antibody green and counterstaining nuclei with Hoechst 33258, cell suspension was added to bioreactors spanned with a porous (A) or nonporous (B) silk microtube coated with SDF-1 $\alpha$ , Matrigel, FBG, and vWF. After 40 h incubation, released platelets were observed in immunofluorescence (Ai, Bi) by confocal analysis only inside porous tubes. As cells were counterstained with Hoechst 33258, we were able to demonstrate that large, nucleated megakaryocytes were not present inside the vascular microtube. Bright field of nonporous (Aii) and porous (Bii) silk microtubes show the tube edges. Yellow dotted lines indicate the tube edges. Color images available online at [www.liebertonline.com/tec](http://www.liebertonline.com/tec)





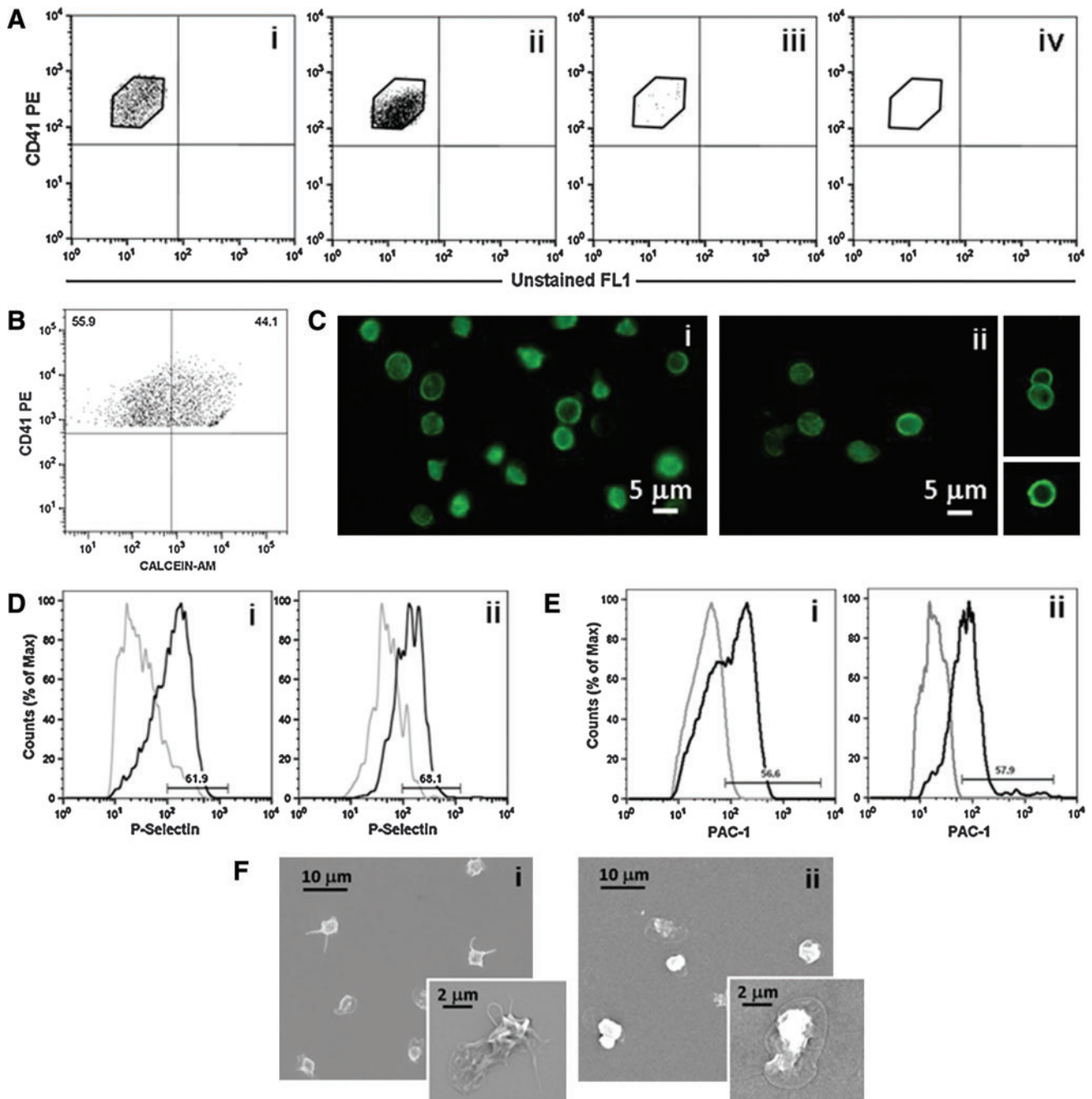


**FIG. 5.** Analysis of collected platelets. **(A)** Flow cytometry analysis of collected platelets in the microtube flow effluent: **(ii)** microtubes coated with SDF-1 $\alpha$  and a combination of Matrigel, FBG, and vWF, **(iii)** uncoated microtubes, and **(iv)** microtubes coated with SDF-1 $\alpha$  and type I collagen. Collected platelets were analyzed as CD41<sup>+</sup> events with the same physical parameters and fluorescence intensity of human blood platelets **(i)**. **(B)** To exclude fragments, collected cells were double-stained with an anti-CD41 antibody and calcein-AM. A representative dot plot is shown. **(C)** Circumferential microtubule coils were observed with an anti-tubulin antibody in the majority of collected platelets **(ii)** when compared to human peripheral blood platelets **(i)**. **(D, E)** Platelets collected after bioreactor perfusion **(Dii, Eii)** revealed increased exposure of P-selectin to the plasma membrane and increased PAC-1 binding after thrombin stimulation, as in human peripheral blood platelets **(Di, Ei)** (gray line indicates unstimulated platelets; black line, thrombin-stimulated platelets). **(F)** Spreading of collected platelets after perfusion **(ii)** was analyzed by SEM in adhesion to type I collagen and compared to human peripheral blood platelets **(i)**. Color images available online at [www.liebertonline.com/tec](http://www.liebertonline.com/tec)

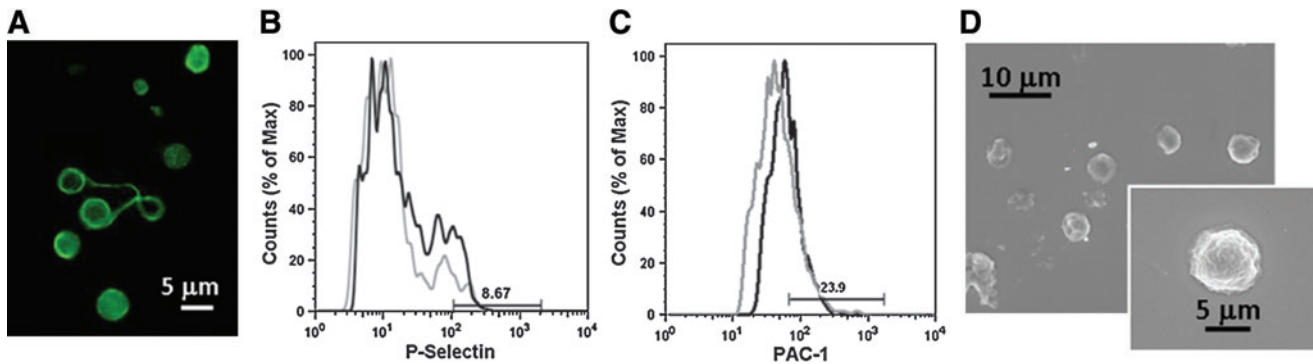


**FIG. 6.** Analysis of *in vitro* released platelets in 2D culture. **(A)** Morphological analysis of *in vitro* released platelets. Immunofluorescence analysis by staining with an anti-tubulin antibody revealed the presence of dumbbells that were still dividing in culture. **(B, C)** Flow cytometry analysis of *in vitro* released platelet functionality. After activation with thrombin, *in vitro* released platelets showed low P-selectin expression **(B)** and PAC-1 binding **(C)** (gray line indicates unstimulated platelets; black line, thrombin-stimulated platelets). **(D)** SEM analysis revealed that the majority of *in vitro* released platelets were not able to spread in adhesion to type I collagen. Color images available online at [www.liebertonline.com/tec](http://www.liebertonline.com/tec)

platelets (Fig. 5Di), collected platelets displayed a slight increase of P-selectin expression in resting conditions.<sup>7</sup> However, expression of P-selectin after thrombin stimulation was comparable in bioreactor collected and control platelets ( $62.7\% \pm 4.1\%$  [mean  $\pm$  SD,  $n=3$ ],  $p>0.05$ ) (Fig. 5Di, ii). Consistently, PAC-1 binding analysis revealed that the activation of the  $\alpha_{IIb}\beta_3$  receptor upon thrombin stimulation was comparable in collected platelets ( $53.1\% \pm 4.8\%$  [mean  $\pm$  SD,  $n=3$ ]) and controls ( $58.1\% \pm 2.1\%$  [mean  $\pm$  SD,  $n=3$ ],  $p>0.05$ ) (Fig. 5E). Finally, collected platelet spreading occurred on type I collagen as shown by SEM analysis (Fig. 5F). Similar spreading was also observed upon adhesion on FBG (data not shown). Altogether, these data pointed out that the 3D bone marrow model allowed the release of functional platelets from megakaryocytes into the perfused vascular tubes.

Interestingly, platelets collected from 2D cultures of human cord blood-derived megakaryocytes differed from both control and 3D bioreactor collected platelets. Specifically, they showed higher variability in size (Fig. 6A), and revealed a significant decrease, as compared to control peripheral platelets, of P-selectin expression ( $6.8\% \pm 1.7\%$  (mean  $\pm$  SD,  $n=3$ ),  $p<0.01$ ) (Fig. 6B) or PAC-1 binding ( $25.6\% \pm 2.4\%$  (mean  $\pm$  SD,  $n=3$ ),  $p<0.01$ ) upon thrombin stimulation (Fig. 6C); most of them failed to spread on type I collagen (Fig. 6D).

## Discussion

Mechanisms underlying relationships between human hemopoietic stem cells and their environment or niche are not well understood. Here we propose a versatile 3D tissue format *in vitro* to establish vascular 3D gel networks in which a bone-like environment can be established<sup>17</sup> and used to further study megakaryocyte functions toward platelet production.<sup>4</sup> This design allows the study of the impact of key environmental variables on subsequent steps of megakaryocyte development toward platelet production. *In vivo* observation of live mice bone marrow suggested that megakaryocytes release large fragments of their cytoplasm into the vasculature.<sup>6</sup> In this context the 3D model of vascular niche was finalized by perfusing the vascular microtubes. While the exact flow rate of bone marrow vasculature is not known, the flow rate in the bioreactor was defined by

taking into account that in capillaries the blood flow shear rate is around  $32/s$ <sup>22</sup> and using the equation by Darby.<sup>23</sup> Many questions are still to be answered regarding the environmental regulation of platelet production. Specifically, how shear stress contributes to platelet release appears to be a key feature yet to be resolved.<sup>6,9,12,27</sup> Whether platelet release occurs totally into the bone marrow space or is completed by fragmentation into circulation or in lung capillary bed represents an intriguing aspect to be unraveled. In this sense our 3D system is a very powerful tool to study the impact of different shear forces on platelet formation as a function of the flow rate applied to the vascular microtubes. Most importantly, our results demonstrate that passage through a vascular-like wall and release into a flowing fluid is a fundamental step to generate functional platelets. Several studies have documented that platelets generated *in vitro* are not fully functional or display an important basal activation state.<sup>7,28–30</sup> The current 3D bioreactor represents a major step forward in strategies of deriving platelets *in vitro*, presumably due to the ability to better emulate native conditions. The system allows for the reproduction of megakaryocyte development that results in the release of more physiological-like platelets. The understanding on how platelets become functional remains to be further elucidated; however, the development of new tools and models to study platelet formation in a more physiologic 3D environment promises that these studies can now go forward. The innovation here is that our 3D model represents the first spatial reconstruction of the bone marrow niche environment.<sup>31</sup> Most importantly, the optical clarity, biocompatibility, low thrombogenicity, non-toxicity and nonimmunogenicity, and compliance of the silk-based tubes make them a unique and useful method for reconstituting vasculature properties to study cell movement across the vascular wall.<sup>15,32</sup>

In conclusion, we envision this 3D bone marrow model as a system to gain new insight into mechanisms of platelet formation. As compared to other bioreactor types used for stem cell migration<sup>33</sup> or for platelet production,<sup>27,28,30,31</sup> our system offers the advantage of combining biochemical parameters, such as different composition of proteins in bone marrow niches, and physical parameters, such as the blood flow. Moreover, our system offers the opportunity to



investigate the subsequence of events that lead to megakaryocyte maturation and the impact of different environmental factors on the release of functional platelets. Altogether these characteristics make our bioreactor a versatile tool in which the different elements of bone marrow environment can be combined to investigate both physiological and pathological megakaryopoiesis. Megakaryocyte-related diseases, such as inherited thrombocytopenias or primary myelofibrosis, are most likely the result of altered regulation of megakaryopoiesis by the bone marrow environment. In this regard, the 3D bioreactor provides a comprehensive model to study, at the same time, different cues of the bone marrow environment related to megakaryocyte development regulation. As a long-term goal, modification of this device in terms of size and number of perfused silk tubes as well as protein coating of vascular tubes and oxygen gradient inside the bioreactor<sup>14,34</sup> may enable the increase of the yield of functional platelets to achieve platelet numbers suitable for clinical applications and use in biotechnology-related industries.

### Acknowledgments

This work was supported by NIH P41 EB002520 (Tissue Engineering Resource Center) and Cariplo Foundation (2006.0596/10.8485), Regione Lombardia—Project SAL-45 and ASTIL 16783-SAL-13, Almamater Foundation (Pavia). We thank Allen Parmelee, Stephen Kwok, Gianluca Viarengo, Cleyton Crepaldi Domingues, Patrizia Vaghi, Alessandro Malara, and Sreevidhya Tarakkad Krishnaji for advice.

### Disclosure Statement

No competing financial interests exist.

### References

- AuBuchon, J.P., Herschel, L., and Roger, J. Further evaluation of a new standard of efficacy for stored platelets. *Transfusion* **45**, 1143, 2005.
- Sullivan, M.T., Cotton, R., Read, E.J., and Wallace, E.L. Blood collection and transfusion in the United States in 2001. *Transfusion* **47**, 385, 2007.
- Avecilla, S.T., Hattori, K., Heissig, B., Tejada, R., Liao, F., *et al.* Chemokine-mediated interaction of hematopoietic progenitors with the bone marrow vascular niche is required for thrombopoiesis. *Nature Med* **10**, 64, 2004.
- Italiano, J.E., Jr., Lecine, P., Shivdasani, R.A., and Hartwig, J.H. Blood platelets are assembled principally at the ends of proplatelet processes produced by differentiated megakaryocytes. *J Cell Biol* **147**, 1299, 1999.
- Becker, R.P., and De Bruyn, P.P. The transmural passage of blood cells into myeloid sinusoids and the entry of platelets into the sinusoidal circulation; a scanning electron microscopic investigation. *Am J Anat* **145**, 183, 1976.
- Junt, T., Schulze, H., Chen, Z., Massberg, S., Goerge, T., *et al.* Dynamic visualization of thrombopoiesis within bone marrow. *Science* **317**, 1767, 2007.
- Reems, J.A., Pineault, N., and Sun, S. *In vitro* megakaryocyte production and platelet biogenesis: state of the art. *Transfus Med Rev* **24**, 33, 2010.
- Takayama, N., Nishimura, S., Nakamura, S., Shimizu, T., Ohnishi, R., *et al.* Transient activation of c-MYC expression is critical for efficient platelet generation from human induced pluripotent stem cells. *J Exp Med* **207**, 2817, 2010.
- Fuentes, R., Wang, Y., Hirsch, J., Wang, C., Rauova, L., *et al.* Infusion of mature megakaryocytes into mice yields functional platelets. *J Clin Invest* **120**, 3917, 2010.
- Balduini, A., Pallotta, I., Malara, A., Lova, P., Pecci, A., *et al.* Adhesive receptors, extracellular proteins and myosin IIA orchestrate proplatelet formation by human megakaryocytes. *J Thromb Haemost* **6**, 1900, 2008.
- Larson, M.K., and Watson, S.P. Regulation of proplatelet formation and platelet release by integrin alpha IIb beta3. *Blood* **108**, 1509, 2006.
- Thon, J.N., Montalvo, A., Patel-Hett, S., Devine, M.T., Richardson, J.L., *et al.* Cytoskeletal mechanics of proplatelet maturation and platelet release. *J Cell Biol* **191**, 861, 2010.
- Sabri, S., Jandrot-Perrus, M., Bertoglio, J., Farndale, R.W., Mas, V.M., Debili, N., *et al.* Differential regulation of actin stress fiber assembly and proplatelet formation by alpha2beta1 integrin and GPVI in human megakaryocytes. *Blood* **104**, 3117, 2004.
- Pallotta, I., Lovett, M., Rice, W., Kaplan, D.L., and Balduini, A. Bone marrow osteoblastic niche: a new model to study physiological regulation of megakaryopoiesis. *PLoS One* **4**, e8359, 2009.
- Lovett, M., Cannizzaro, C., Daheron, L., Messmer, B., Vunjak-Novakovic, G., *et al.* Silk fibroin microtubes for blood vessel engineering. *Biomaterials* **28**, 5271, 2007.
- Lovett, M.L., Cannizzaro, C.M., Vunjak-Novakovic, G., and Kaplan, D.L., Gel spinning of silk tubes for tissue engineering. *Biomaterials* **29**, 4650, 2008.
- Yin, T., and Li, L. The stem cell niches in bone. *J Clin Invest* **116**, 1195, 2006.
- Kim, U.J., Park, J., Li, C., Jin, H.J., Valluzzi, R., *et al.* Structure and properties of silk hydrogels. *Biomacromolecules* **5**, 786, 2004.
- Li, C., Vepari, C., Jin, H.J., Kim, H.J., and Kaplan, D.L. Electrospun silk-BMP-2 scaffolds for bone tissue engineering. *Biomaterials* **27**, 3115, 2006.
- Patel, S.R., Hartwig, J.H., and Italiano, J.E., Jr. The biogenesis of platelets from megakaryocyte proplatelets. *J Clin Invest* **115**, 3348, 2005.
- Bourke, V.A., Watchman, C.J., Reith, J.D., Jorgensen, M.L., Dieudonné, A., *et al.* Spatial gradients of blood vessels and hematopoietic stem and progenitor cells within the marrow cavities of the human skeleton. *Blood* **114**, 4077, 2009.
- Cortinovis, A., Crippa, A., Cavalli, R., Corti, M., and Cattaneo, L. Capillary blood viscosity in microcirculation. *Clin Hemorheol Microcirc* **35**, 183, 2006.
- Darby, R. *Chemical Engineering Fluid Mechanics*, 2 ed. Boca Raton, FL: CRC Press, 2001, p. 64.
- Sabri, S., Foudi, A., Boukour, S., Franc, B., Charrier, S., *et al.* Deficiency in the Wiskott-Aldrich protein induces premature proplatelet formation and platelet production in the bone marrow compartment. *Blood* **108**, 134, 2006.
- Dhanjal, T.S., Pendaries, C., Ross, E.A., Larson, M.K., Protty, M.B., *et al.* A novel role for PECAM-1 in megakaryocytopoiesis and recovery of platelet counts in thrombocytopenic mice. *Blood* **109**, 4237, 2007.
- Nurden, P., Gobbi, G., Nurden, A., Enouf, J., Youlyouzmoufak, I., *et al.* Abnormal VWF modifies megakaryocytopoiesis: studies of platelets and megakaryocyte cultures from patients with von Willebrand disease type 2B. *Blood* **115**, 2649, 2010.

27. Dunois-Lardé, C., Capron, C., Fichelson, S., Bauer, T., Cramer-Bordé, E., *et al.* Exposure of human megakaryocytes to high shear rates accelerates platelet production. *Blood* **114**, 1875, 2009.
28. Sullenbarger, B., Bahng, J.H., Gruner, R., Kotov, N., and Lasky, L.C. Prolonged continuous *in vitro* human platelet production using three-dimensional scaffolds. *Exp Hematol* **37**, 101, 2009.
29. Takayama, N., Nishikii, H., Usui, J., Tsukui, H., Sawaguchi, A., *et al.* Generation of functional platelets from human embryonic stem cells *in vitro* via ES-sacs, VEGF-promoted structures that concentrate hematopoietic progenitors. *Blood* **111**, 5298, 2008.
30. Matsunaga, T., Tanaka, I., Kobune, M., Kawano, Y., Tanaka, M., *et al.* *Ex vivo* large-scale generation of human platelets from cord blood CD34+ cells. *Stem Cells* **24**, 2877, 2006.
31. Di Maggio, N., Piccinini, E., Jaworski, M., Trumpp, A., Wendt, D.J., *et al.* Toward modeling the bone marrow niche using scaffold-based 3D culture systems. *Biomaterials* **32**, 321, 2009.
32. Omenetto, F.G., and Kaplan, D.L. New opportunities for an ancient material. *Science* **329**, 528, 2010.
33. de Barros, A.P., Takiya, C.M., Garzoni, L.R., Leal-Ferreira, M.L., Dutra, H.S., *et al.* Osteoblasts and bone marrow mesenchymal stromal cells control hematopoietic stem cell migration and proliferation in 3D *in vitro* model. *PLoS One* **5**, e9093, 2010.
34. Lovett, M., Rockwood, D., Baryshyan, A., and Kaplan DL. Simple modular bioreactors for tissue engineering: a system for characterization of oxygen gradients, human mesenchymal stem cell differentiation, and prevascularization. *Tissue Eng Part C Methods* **16**, 1565, 2010.

Address correspondence to:

David L. Kaplan, Ph.D.

Department of Biomedical Engineering

Tufts University

4 Colby St.

Medford, MA 02155

E-mail: david.kaplan@tufts.edu

Alessandra Balduini, M.D.

Biotechnology Research Laboratories

Department of Biochemistry

IRCCS San Matteo Foundation

University of Pavia

via Bassi 21

27100 Pavia

Italy

E-mail: alessandra.balduini@tufts.edu;

alessandra.balduini@unipv.it

Received: March 4, 2011

Accepted: July 25, 2011

Online Publication Date: September 5, 2011